BULLETIN OF THE POLISH ACADEMY OF SCIENCES
TECHNICAL SCIENCES
DOI: 10.24425/bpasts.2024.150808

THIS IS AN EARLY ACCESS ARTICLE.
This article has been accepted for publication in a future issue of this journal,
but has not been fully edited. Content may change prior to final publication.

Performance Evaluation of 5G New Radio Low Density Parity Check Codes over Different Scenarios of Lognormal Fading Channel

Mohammed Hussin Ali[1], Ghanim A. Al-Rubaye[1]

[1] Electrical Engineering Department, College of Engineering, Mustansiriyah University, Baghdad, Iraq

Abstract. Low Density Parity Check (LDPC) is a channel coding technique widely utilized in the 5G New Radio standard, it is of utmost importance in facilitating proficient and secure communication in noisy environments by effectively minimizing errors during data transmission. It is primarily used in the 5G New Radio (NR) standard for encoding user information on the Physical Downlink Shared Channel (PDSCH). The necessity to satisfy the increasing expectations for throughput, latency, and dependability led to the decision to deploy LDPC codes for user data, especially in the enhanced mobile broadband (eMBB) and ultra-reliable and low-latency communications (URLLC) scenarios of 5G networks. The present system proposes the use of NR-LDPC codes for the purpose of transmitting data across a lognormal multipath fading channel model in the presence of AWGN. Wireless communication channels often use a lognormal multipath fading channel model, where the received signal experiences both multipath fading and lognormal shadowing. The research investigates the effectiveness of NR-LDPC coding in improving QAM-OFDM system performance by analyzing two rate-compatible base graphs and comparing their effectiveness with an uncoded system. This analysis is crucial for optimizing communication network design, especially in scenarios where the integrity of data is of utmost importance. We introduce a new method to improve the 5G NR LDPC code capability under lognormal fading conditions. This approach develops a layered Min Sum (LMS) algorithm to provide enhanced error correcting capabilities. The developed and implemented decoding algorithm represents a significant advancement over traditional detection methods. The outcomes of the simulation provide evidence of the effectiveness of the proposed NR-LDPC coding techniques in terms of their error correction and identification capabilities. In addition, the developed LMS decoding algorithm has been shown to significantly decrease the BER of the system.

Key words: QAM, OFDM, NR-LDPC, Lognormal Fading Channel, BER, 5G NR, Physical Uplink Shared Channel (PUSCH), Physical Downlink Control Channel (PDCCH), Enhanced Mobile Broadband (eMBB), LTE-advanced (LTE-A).

1. INTRODUCTION

Wireless communications of the 5G are estimated to provide for a variety of scenarios. Wireless communication in high mobility conditions, such as fast speeds railroads and drones Unmanned Aerial Vehicle (UAVs), is considered a critical situation. Nevertheless, the significant mobility frequently results in substantial Doppler shift, hence posing significant challenges to the reliability of wireless communications. Various strategies have been explored to facilitate high mobility communications. The coding of channels is a core part of any communication network. Future wireless systems will require powerful algorithms with low-complexity encoding and decoding in order to meet a wide variety of requirements, from running in highly dependable situations with simple informational messages along with low coding rates for operating in situations requiring high throughput, long messages, and high coding rates. Utilizing, **Low** Density Parity Check (LDPC) codes is mostly seen in the Physical Downlink Shared Channel (PDSCH) of the Fifth Generation New Radio (5G NR) standard [1]. The selection of LDPC codes algorithm for client data and utilize Polar codes for control data, particularly in the context of Enhanced Mobile Broadband (eMBB), and Ultra-Reliable Low Latency Communications (URLLC) scenarios, was motivated by the objective of achieving the demands for enhanced throughput, reduced latency, and improved reliability in 5G systems [1-2]. LDPC codes have become known for their robust error-correcting capabilities and are highly suitable for scenarios with high data flow, such as eMBB. The ability to accurately resolve inaccuracies in the received data significantly contributes to guaranteeing the dependable transfer of user data through the PDSCH.

LDPC codes have significance for ensuring fast and reliable communication in a noisy channel environment because they aid in lowering data transmission errors. An earlier version of the LDPC code was first presented in [3], has undergone extensive development over an interval of many decades. It has found significant use in several wireless communication contexts, including profound space communications [4],

*e-mail: eeph005@uomustansiriyahy.edu.iq

This article has been accepted for publication in a future issue of this journal, but has not been fully edited. Content may change prior to final publication.

Digital Terrestrial TV Broadcasting (DTTB) [5-8], and Wireless Local Area Networks (WLANs) [9]. One of the major technological advances in 5G NR is the introduction of LDPC code utilized for channel coding technique for the data channel, where Turbo coding was used in Fourth Generation Long- Term Evolution (4G LTE and Long- Term Evolution - Advanced (LTE-A) networks is now replaced [4]. Orthogonal Frequency Division Multiplexing (OFDM) is a widespread modulation technique utilized by wireless communication networks. The operational approach is the division of an extremely fast data stream into many streams with reduced data rates. These streams are then sent simultaneously using a set of closely spaced subcarriers. OFDM is well recognized for its ability to diminish the negative impacts of interference from multiple directions and frequency-selective fading, making it a wise option for achieving high speeds of data transfer in diverse wireless communication technologies, such as 5G. The use of NR-LDPC-coded OFDM in the area of 5G and Beyond Fifth Generation(B5G) integrates the advantageous features of OFDM modulation with LDPC coding, hence enhancing error correction capabilities. In challenging wireless scenarios, this technology facilitates the achievement of high data transmission rates, reduced latency, and reliable connectivity. Comparing the LDPC codes to other iterative codes like turbo codes, they are fundamentally simpler and provide a fully parallelizable decoding implementation [10]. In general, turbo codes (TCs) contain complicated code structures, a significant delay in the decoding process, and other characteristics that make TCs inappropriate for 5G. LDPC codes provide superior performance and need less bandwidth, particularly when used to longer block lengths. According to reference [11,12], LDPC codes exhibit higher efficiency compared to other coding schemes. Iterative soft-decision decoding of LDPC codes provides performance that is almost equivalent to the Shannon limit. Additionally, it offers reduced decoding complexity and allows for simple modification of code rates, resulting in improved BER performance compared to turbo codes [13].

Recently, a lot of approaches have been used to improve the error-correction performance of 5G LDPC codes [14–19]. The modified minimum sum (MS) and algorithms that provide an extended approximation to the minimum value were introduced by [14] and then [15]. By considering the approximate-min approach as described in reference [16]. The author in [17], improves the performance of the 5G NR system by employing the MS approach on the base matrix ($BG1$) within the decoder for LDPC, specifically focusing on 5G standards, and increasing iterations, especially for larger code words. A significant level of implementation complexity is required for non-linear functions like the BP decoding. In order to streamline the non-linear functions inside the BP approach, a hybrid decoding methodology was introduced by the researchers of [18]. In order to enhance the precision of the calculations, the authors mentioned in [19] include offset and normalization factors into the decoding process at certain intervals. These variables are carefully adjusted using machine learning methods. Layered decoding algorithms may be used with Normalized Min-Sum (NMS) or Offset Min-Sum (OMS) algorithms to achieve an optimal equilibrium between BER, decoding complexity, and decoding convergence time [20].

Optimal use of the available spectrum may be achieved by the implementation of the OFDM communication technology. In this particular configuration, the usage of the spectrum may be significantly enhanced by using M-ary Quadrature Amplitude Modulation (M-QAM). Nevertheless, in some scenarios, the use of high-order modulation techniques may result in a significant increase in error rates for low-power transmission systems. Forward Error Correction (FEC) is often used in OFDM technique to diminish the occurrence of errors [21- 22]. OFDM is typically used in combination with a cyclic prefix (CP) to remove inter-symbol interference (ISI), which transforms frequency-selective channels into narrow-band frequency-flat fading channels.

In our research, we have developed and implemented an NR-LDPC-QAM-OFDM system, and subsequently evaluated and compared its Bit Error Rate (BER) performance with that of uncoded QAM-OFDM systems over a multipath lognormal environment and in an Additive White Gaussian Noise (AWGN).. The findings of our research indicate that the NR-LDPC-COFDM system exhibits superior performance compared to the uncoded OFDM system in a multipath channel scenario characterized by progressive channel degradation. The LPDC-OFDM convergence requires a larger number of iterations, which is considered a significant limitation. On the other hand, the NR-LDPC technique has the capability to reduce the necessary decoding iterations for correcting channel errors by around 18-29% at a moderate Signal-to-noise ratio. This article presents a comprehensive examination of the computation of BER in the context of a Lognormal Fading Channel (LFC). The LFC is a commonly used theoretical framework within the domain of wireless communication systems. It is crucial to comprehend the BER achievement inside such channels in order to develop communication systems that are both dependable and efficient.

The subsequent parts of the article are organized according to the following structure: Section II of the LDPC Code provides a comprehensive contextual foundation by demonstrating the techniques in more detail. This portion of the article provides an explanation of the 5G NR LDPC Code system.

Part III details the NR-LDPC-COFDM system's design and implementation framework, pertaining to the system. The computation of BER involves evaluating the error probability for each sent bit, taking into account the channel characteristics and the modulation scheme used within Section IV. While Section V provides a quantitative evaluation of LDPC-COFDM systems, presenting simulation results as empirical evidence of their performance. The last section of the document summarizes the findings and implications.

2. 5G NR LDPC TECHNIQUES

Every possible channel in the physical world introduces unwanted noise, which in turn causes errors and lowers the system's dependability. Channel coding improves the dependability of wireless communication networks by adding

This article has been accepted for publication in a future issue of this journal, but has not been fully edited. Content may change prior to final publication.

redundancies to transmit information in an organized manner. One subclass of linear block codes are LDPC codes, denoting that their whole specification may be determined just via their generating matrix G and H which is parity matrix H. The sparsity of these codes is one noteworthy feature, characterized by a reduced quantity of elements that are non-zero inside the H [23].

The codes from the LDPC process may be categorized into two separate groups: regular and non-regular. The popularity of LDPC code has increased significantly as a result of its ability to achieve large throughputs, reduced decoding complexity, and better decoding latency. This is specifically advantageous within the framework of handling information with 5G technology. The protograph architecture used by the 5G-NR specifications encompasses many crucial aspects. Two basic graphs are available., namely $BG1$ as well as $BG2$ [24]. Various modifications such as Z_C, and techniques including shortening and puncturing to achieve various rates [25-26]. In the context of the 5G standard, a protograph is often denoted by a base graph structure [27]. The usage of a system is determined by either the coding rate or the quantity of information bits. The size of the transport block being transferred over the PDSCH determines which base graph is used, with $BG1$of a size of (46 x 68) being when the size of the transit block surpasses a certain threshold, and $BG2$ of a dimension (42 x 52) being employed when the transfer block size is below this threshold. The $BG2$, being smaller in size, is considered more appropriate for shorter transport blocks due to its ability to strike a more favorable balance between complexity and efficiency.

The first 10 columns of $BG1$ have a total of 22 information bits, whereas the first ten columns of $BG2$ contain 10 data bits. It is crucial to consider the initial pair of columns for both BGs are consistently perforated and don't engage in any activity in the transmission process. The generation of H of protograph codes may be achieved by replacing every zero-valued component of the BG with a $(Zc \times Zc)$ all zero matrix and substituting every component has a value of zero by a $(Zc \times Zc)$ matrix of permutations. The term "lifting size," denoted as Zc, pertains to the quantity of attached copies of the protograph [28]. A total of 51 distinct lifting sizes have been specified. The variable Zc is typically used to represent this concept, and its value can be determined by employing eq. (1) with the given index and the maximum value provided by the Z_c is 384 as shown in Eq. (1) [29-30].

$$Z_c = d \times 2^{i_{LS}} \quad (1)$$

The index i_{LS} range from 0 to I_d, while d is a number selected from the set (2, 3, 5, 7, 9, 11, 13, 15), and the value of $I_d \in$ (7, 7, 6, 5, 5, 5, 4, 4). which value is determined based on the index number (0, 1, 2, 3, 4, 5, 6, 7). One of the main benefits of utilizing a matrix of identities with a cyclic shift as a PM (permutation matrix) is that it allows each permutation to be represented by a single integer.

2.1. 5G NR LDPC Encoder

The LDPC of (N, K) code is composed of a codeword with a length of N bits, a message length of K bits, and $(N - K)$ parity bits. The LDPC matrix, denoted as H, is a sparse matrix with dimensions $(N - K) * N$, where $N * (N - K)$ is the formula for calculating the overall number of entries. The use of two distinct base graphs throughout the encoding process serves the purpose of accommodating varied code rates. The primary use of the $BG1$ is for accommodating greater lengths of user data blocks within the 500–8448 range. Additionally, it is utilized to enable a very high rate of code variation, ranging from 1/3 to 8/9. The $BG2$ is utilized for short lengths of user data within the 40 to 2560 range, which is considered appropriate for lower variable rates ranging from 1/5 to 2/3 [31-32].

The data on the traffic channel is encoded by the LDPC coder by extending the message bits with parity bits. In order to ensure the safety of the data, a Cyclic Redundancy Check (CRC) encoder segments the data into smaller blocks and attaches a CRC to each one. Rate-matching procedures might include either puncturing or shortening as shown in Fig.1. The technique of encoding the LDPC code relies heavily on the H, that is expanding upon the base matrix. The encoder is responsible for calculating the parity bits using a matrix operation. Lengths K, N - K, and N of the array vector are, message $m = m_1, m_2, \ldots . m_K$, parity $p = p_1, p_2, \ldots . p_{(N-K)}$, and codeword $C = C_1, C_2, \ldots C_{(N-K)}$

The codeword C that may be typed by eq. (2) contains both the information and the computed parity.

$$C = m_1, m_2, \ldots . m_K, p_1, p_2, \ldots . p_{(N-K)} \quad (2)$$

In order to get the correct codeword, which includes the data and specifies the process conducted on the data portion to compute the parity bits (p) , the H and codeword must meet Eq. (3).

$$[H] * [C^T] = 0 \quad (3)$$

The preceding equation may be simplified to Eq. (4) by decomposing the H into its P component and its I identity component.

$$[P \ I] \begin{bmatrix} m^T \\ P^T \end{bmatrix} = 0 \quad (4)$$

The complex doubling diagonal matrix of the H is used to identify the first four parity bits in the 5G standard, whereas the I of the H is utilized to determine the fifth and terminal parity bits.

2.2. 5G NR LDPC Decoder

Due to its simple implementation and straightforward decoder, LDPC codes operate near to their maximum capacity. Since the LDPC decoders employ soft-in soft-out (SISO) algorithms, the information sent by the decoders is a probability of the actual channel data that are received. The message is frequently delivered through the Check Nodes (CNs) and the Variable Nodes (VNs) via SISO decoder the decoder employs an iterative approach to estimate the actual values of the channel, bits one by one, based on the received vector. It utilizes the full incoming vector together with information from the bit that has been previously decoded to estimate the subsequent bits. The internal transmission of information is facilitated by utilizing the LLR [33].

At the first iteration, the LDPC decoder utilized the intrinsic information of the channel, and intrinsic information was

This article has been accepted for publication in a future issue of this journal, but has not been fully edited. Content may change prior to final publication.

calculated for each of the received values independently; which corresponded exactly to the received value of the AWGN channel. [34]. The LLR value can be determined as Eq. (5)

$$\mathcal{L}i = \mathcal{L}\log\left(\frac{P_r\left(c_i=\frac{0}{y_i}\right)}{P_r\left(c_i=\frac{1}{y_i}\right)}\right) = \mathcal{L}og\left(\frac{g\left(\frac{y_i}{c_i}=0\right)}{g\left(\frac{y_i}{c_i}=1\right)}\right) = \mathcal{L}\log\left(\frac{e^{2y_i}}{\sigma^2}\right) \quad (5)$$

Where $\mathcal{L}i$ represents LLR intrinsic information, which is initial knowledge or belief about the bits to be decoded. While c_i represent the i^{th} bit of [C] while y_i represent the i^{th} bit of received value. After being simplified, Eq. (5) yields the ultimate $\mathcal{L}i$ value, as seen in Eq. (6).

$$\mathcal{L}i = y_i * \left(\frac{2}{\sigma^2}\right) \quad (6)$$

The extrinsic LLR ($\mathcal{L}_e$) output provides the belief of specific bits inside the incoming vector y. The use of the term "afterword" after the first iteration in the decoder of LDPC is feasible, as shown by Eq. (7).

$$\mathcal{L}_e = \mathcal{L}\log\left(\frac{e^{[2*(y_1+y_2+y_3+\cdots+y_N]}}{\sigma^2}\right) \quad (7)$$

where $y = \{y_1, y_2, y_3 \ldots y_N\}$is represent the whole received vector. By eliminating the exponential term using logarithm

$$\mathcal{L}_e = (y_1 + y_2 + y_3 + \cdots + y_N)\left(\frac{2}{\sigma^2}\right) \quad (8)$$

The term $\left(\frac{2}{\sigma^2}\right)$ is a positive factor and may be disregarded. Utilizing the (tanh) function, one may effectively express the calculation of the conditional $\mathcal{L}_e$ immediately after the application of the expectation operation in iterative decoding algorithms, such turbo codes, as in Eq. (9)

$$g(x) = \mathcal{L}\log\left(tanh\left(\frac{|x|}{2}\right)\right) \quad (9)$$

An accurate way to estimate the final result of a log(tanh) function is to use a basic min-sum algorithm.

$$g(x,y) = sign(x) * sign(y) * \min(|\boldsymbol{x}|, |\boldsymbol{y}|) \quad (10)$$

The rows of the Parity Check Matrix (PCM) are partitioned into multi layers using the layered min-sum technique [35–37], also known as the layering. The process of layering is executed in a manner that ensures that each layer in the PCM has a column weight of one. The layered min-sum decoder (LMND) achieves superior error performance and requires less iterations, while also exhibiting more rapid convergence. As shown in Fig. 1, The initial decoder utilized the LLR for the first iteration, and then applied the $\mathcal{L}_e$ on subsequent iterations. The LMND employs an iterative process in which the decoders of each layer take turns updating the belief, and the final decoder makes an estimate based on the updated belief to produce the estimated decision. Subsequently, as the initial step in the process of layering, matrices are generated for each respective set. The two layers:

$$H = \begin{bmatrix} H_1 \\ H_2 \end{bmatrix} \quad then \quad \mathcal{L} = \begin{bmatrix} \mathcal{L}_1 \\ \mathcal{L}_2 \end{bmatrix}$$

In the initialization stage as the second step, the vector y_j is utilized to modified the matrix $\mathcal{L}_1$.

$$\mathcal{L}_1[:,j] = y_j \quad \text{for } \mathcal{L}_1[:,j] \neq 0$$

where $j = 1,2, \ldots \ldots \ldots \ldots, N$

Following the initialization step, a min-sum (MS) method utilized the single parity check (SPC) algorithm for the decoder to carry out a row operation on each row of the PCM.

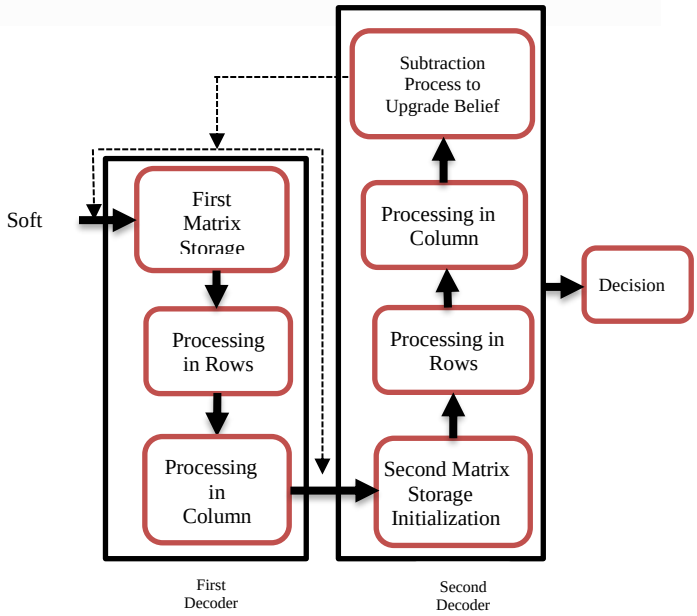

Fig.1.Layered min-sum decoder

This task required the identification of the two smallest values, min1 and min 2, as well as the determination of the location of min1in the vector "POS." The sum of all the values in the y_j vector is computed, referred to as parity (Ꝑ). The aforementioned procedure is executed on the CNs inside the $\mathcal{L}$ matrix.

$\mathcal{L}_{[:,1:j]} = min_2$ when $\mathcal{L}[i,j] \neq 0$

$\mathcal{L}_{[:,Pos]} = min_1$ when $\mathcal{L}[i,j] \neq 0$

The sign of $\mathcal{L}_{New} = \mathcal{L}(\text{sign}) * Ꝑ$

In the next step, the MS approach utilizes the repetition code to construct a new vector by means of addition for each column of the PCM . The VNs are updated by performing the following column process Assisted by the matrix $\mathcal{L}$ and the whole vector y_j, to adjust the belief:

$S_j = y_j + S(\mathcal{L}_1[:,j])$

The sign of $\mathcal{L}_{New} = \mathcal{L}(\text{sign}) * Ꝑ$

In the next step, the MS approach utilizes the repetition code to construct a new vector by means of addition for each column of the PCM . The VNs are updated by performing the following column process Assisted by the matrix $\mathcal{L}$ and the whole vector y_j, to adjust the belief:

$S_j = y_j + S(\mathcal{L}_1[:,j])$

Then executed a column operation on $\mathcal{L}_2$

$$S_j = y_j + S(\mathcal{L}_2[:,j])$$

Update the summation of the variable S_j from the first level of the given data set $\mathcal{L}_1$.

$$S_j = S_j - S(\mathcal{L}_1[:,j])$$

Update the summation of the variable S_j from the first level of the given data set $\mathcal{L}_2$.

$$S_j = S_j - S(\mathcal{L}_2[:,j])$$

This article has been accepted for publication in a future issue of this journal, but has not been fully edited. Content may change prior to final publication.

Finally, by utilizing a hard decision, the Min-Sum strategy predicts the ultimate codeword at a threshold of zero.

$$d_k = g(x) = \begin{cases} 0, & S_j > 0 \\ 1, & S_j < 0 \end{cases} \quad (11)$$

From one decoder to another, the " Enhancement of the Subtract-Min-Sum algorithm " process is carried out via the LMS algorithm. The LMS technique exhibits an equilibrium between computational speed as well as effectiveness as a result of suboptimal stacking implementations.

3. 5G NR LDPC-COFDM SYSTEM MODEL

The architecture of our 5G NR LDPC-COFDM system is shown in Fig. 2. In the subsections that follow, we'll break down the main parts of the system's block diagram and explain what it does.

3.1Transmitter.

The system's transmitter con comprises an LDPC encoder, an M-QAM modulator, an Inverse Fast Fourier Transform (IFFT) portion, and a CP block. The input is supposed to have a perfectly random and statistically independent order of bits.

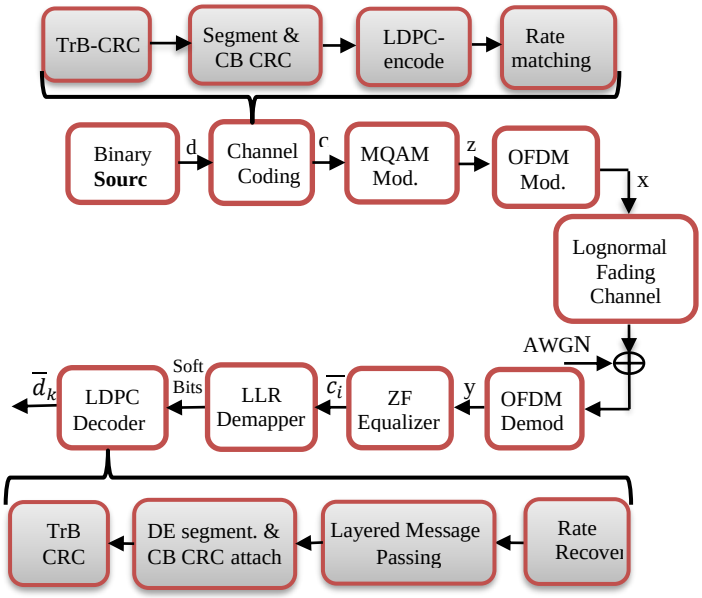

Fig. 2. Schematic structure NR-LDPC Code QAM-OFDM

The input sequence of bits ($d = d_0, d_1,..., d_{k-1}$) is encoded by utilizing an LDPC code. Both capacity-approaching codes have the same encoding rate of 0.5, and 0.333. The output of the NR-LDPC encoder($c_i = c_o, c_1, \ldots, c_{n-1}$), is sent into a digital modulator, where it is rearranged into various patterns, such as the 4-QAM format, where two coded bits are merged to make a single symbol. Just as how one 16-QAM symbol is generated by combining four groups of coded bits. Under the gray mapping constellation, the bits that are coded are joined to create the matching symbol, Therefore, the appropriate QAM symbol for a K-tuple $\{ c_m, c_{m+1},... c_{m+k+1} \}$ of bits, is,

$$X_k = \boldsymbol{C}\left[\sum_{m=0}^{k-1} 2^{k-1-m}\, c_m\right] \quad (12)$$

The symbol $\boldsymbol{C} \in \mathbb{C}^{1x2^k}$ represents the vector of Gray-encoded in the time domain. Using a mapping to M symbols, the rate matched bits of information are partitioned into collections of m=log2(M) bits. Mapping points of constellations may be utilized to create symbols of QAM with length $\mathcal{N}$=E/m . A serial-to-parallel converter receives the digitally modulated symbol of code bits c_i and makes it possible to process the symbols c_i in parallel that is in a serial fashion. The frequency domain is therefore represented by the symbols c^f[i] where i = 1, 2,.... When an IFFT is applied, the signal that comes out is the time domain signal that corresponds to $, c^t$ [i] to facilitate transmission, the parallel signal is c^t [i] returned to its serial form after conversion.

An N-points IFFT may be used to create a complex OFDM signal in the baseband, may be expressed as

$$x_n = \frac{1}{\sqrt{\mathcal{N}}} \sum_{k=0}^{N-1} X_k \exp\left(\frac{2j\pi kn}{\mathcal{N}}\right), \quad n = 0,1, \ldots, \mathcal{N}-1 \quad (13)$$

is shown in Eq. (13) [38]. The phenomenon of Inter-Symbol Interference (ISI) resulting from multipath propagation has affected the entire conventional wireless communication systems. A CP with a duration of $\mathcal{N}_{CP}$ data sets samples is employed, which is introduced at the onset of OFDM symbol via duplicating the final $\mathcal{N}_{CP}$ samples obtained from IFFT output x_n and inserting them to the start of x_n, which aims to surpass the max. dispersion delay of the fading channel (L_d). As a result, the transmitted symbols $\tilde{x}$=[$x_{N-N_{CP}}$, $x_{N-N_{CP}+1}$,...,$x_{\mathcal{N}}$, $x_o, x_1, \ldots, x_{\mathcal{N}-1}$], are generated , which have a total length of $\mathcal{N}_t = \mathcal{N} + \mathcal{N}_{cp}$ samples . This technique effectively reduce the influence of ISI that occurs between consecutive OFDM signals within channels. The aforementioned carriers traverse a diverse range of fading channels, whereby each channel introduces its own distinct noise at the point of reception. This noise contributes to the signal as shown in Eq. (14).

3.2 Multipath Channel Model.

Fundamental to the work of communication theory is the assumption of some degree of noise distortion in transmitted signals. In most cases, it is supposed that the noise is AWGN. A more practical situation for wireless communications is when transmitters and receivers may be connected via multiple paths. These paths may be straight or generated by processes including reflection, diffraction, and scattering. The gathered signal is a vector of individual delayed signals, each of which has its own frequency, amplitude, and delay [39].

For short-term or localized fades, the Rayleigh and Rician distributions are useful, but the lognormal distribution is better suited to explain longer-term or worldwide occurrences. On the other hand, Nakagami's m-distribution [40] is a more adaptable statistical model that can replicate both the Rayleigh and the one-sided Gaussian fading scenarios. Furthermore, at certain intervals on the mean rating scale, the Nakagami distribution may serve as a suitable approximation to the Rician and log-normal distributions [38].

The Nakagami and Rician distributions are a better fit for low signal-to-noise levels (SNRs) than they are for high SNRs.

This article has been accepted for publication in a future issue of this journal, but has not been fully edited. Content may change prior to final publication.

The Nakagami distribution also gives a better fit to experimental data over a broad range of propagation in the physical channels, and it is more flexible than the log-normal and Rician distributions [38]. The performance of a system will suffer greatly if fading occurs.

The flat fading channel model is the one that is used the most often for limited bandwidth transmission via mobile and wireless channels. The flat fading channel reduces the strength of all of the individual frequency elements that make up the signal equally. Because of this, the received signal, which was in its complex baseband form, may be expressed as [41], [42]

$$\mathcal{Y} = \beta\mathcal{X} + \mathcal{U} \quad (14)$$

$\mathcal{Y}$ represents the signal that was received and $\mathcal{X}$ represents the symbol that was sent, $\mathcal{U}$, is AWGN amplitude, and β is the fading channel coefficients. A stochastic function is the amplitude of the fade, which is represented by the symbol " β " The channel exhibits nothing but AWGN when there is no fading at all (β = 1).

If the amplitude of the fading channel adheres to the Rayleigh distribution, then the probability distribution $P(|\beta|)$ may be written as the following [43]

$$f_\beta(\beta) = \frac{\beta}{\sigma_h^2}\exp\left(-\frac{\beta^2}{2\sigma_h^2}\right) \quad (15)$$

In this situation, the inphase and quadrature phase components will both have distributions that are Gaussian with N (0, 1/2) as:

$$f_\beta(\beta^I) = \frac{1}{\sqrt{2\pi\sigma_h^2}}\exp\left(-\frac{(\beta^I)^2}{2\sigma_h^2}\right), \quad -\infty \le \beta^I < \infty \quad (16)$$

$$f_\beta(\beta^Q) = \frac{1}{\sqrt{2\pi\sigma_h^2}}\exp\left(-\frac{(\beta^Q)^2}{2\sigma_h^2}\right), \quad -\infty \le \beta^Q < \infty \quad (17)$$

Where σ_h^2 indicate to the typical strength of the signal that has been received, which is based on the path of loss and the shadowing alone.

The quality of the connection may be negatively impacted in terrestrial and satellite land-mobile systems by the gradual variation in the average mean signal strength that are brought on by the shadowing that is caused by topography, buildings, and trees. The performance of the communication system will only be dependent on the influence of shadowing if the radio receiver has the capability to mitigate the fast fluctuations caused by multipath fading via averaging, or if the impacts of multipath are mitigated by employing a reliable diversity network. On the basis of actual observations, there is widespread agreement that shadowing may be represented by log-normal distribution for a variety of situations, both indoor and outdoors [44-46]. In this scenario, the route SNR per symbol β will have a Probability Density Function(PDF) that is provided by the conventional log-normal equation. Consequently, the amplitude of the fading in the time domain follows the log-normal distribution and is described as

$$f_\beta(\beta^\Upsilon) = \frac{\Lambda}{\beta^\Upsilon\sqrt{2\pi}\sigma}\exp\left(-\frac{(10\log_{10}\beta^\Upsilon - m)^2}{2\sigma^2}\right), \quad (18)$$

The Eq. (18), which can alternatively be represented as

$$f_\beta(\beta^\Upsilon) = \frac{1}{\beta^\Upsilon\sqrt{2\pi\sigma^2}}\exp\left(-\frac{(\ln\beta^\Upsilon - m)^2}{2\sigma^2}\right), \quad (19)$$

where $0 \le \beta^\Upsilon < \infty$

where $\beta^\Upsilon > 0$, and $\Upsilon = \{\mathcal{I}, \mathcal{Q}\}$ indicate to the real component and imaginary component, respectively.

The parameters m and σ represent the average mean and standard deviation, respectively, of the logarithm of β^Υ. It is possible to represent those parameters in dB, as $\sigma = \sigma_{dB}/\Lambda$ and $m = m_{dB}/\Lambda$, where the value $\Lambda = \frac{10}{ln10}$ =4.3429[47. The PDF of the variable in decibels will be Gaussian if the lognormal variable is changed to decibel units. One may represent the parameter m in terms of average Signal to Noise Ratio(SNR), in such a way $m_{dB} = \beta^\Upsilon - \frac{\sigma_{dB}^2}{\Lambda}$. For the majority of wireless network communication regimes over channel has log-normal distribution, the σ_{dB}, parameter sometimes referred to as the dB spread, has been observed fluctuate within a certain range of 1–12dB [48]. For the actual dB spread in mobile communication, Fig. 3 displays the PDF plot and the typical SNR (β^ΥdB). After performing an FFT function, the distribution of the channel distribution's real and imaginary parts in Eqs. (18) or (19) will become closer and closer to a normal distribution, as stated by the Central Limit Theorem (CLT), i.e. $f_\beta(\beta^\Upsilon) = N(\beta^I, 0, {\sigma_{LN}}^2)$ and $f_\beta(\beta^\Upsilon) = N(\beta^Q, 0, {\sigma_{LN}}^2)$ where β^I and β^Q are zero-mean statistically independent orthogonal Gaussian R.V. utilizing the value of Eq.(19) to determine the variance.

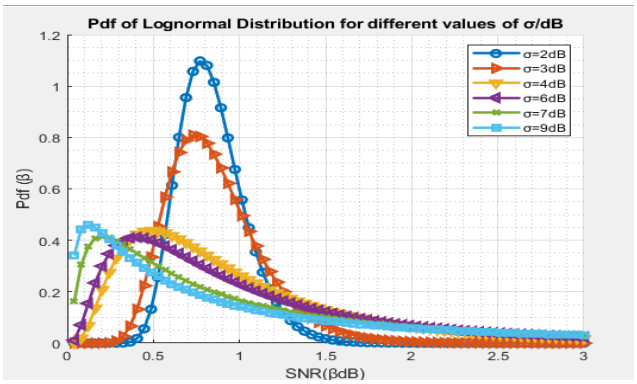

Fig.3. PDF of an instantaneous SNR for different σdB values with mdB=1

$${\sigma_{LN}}^2 = E\{|\beta^\Upsilon|^2\} - (E\{|\beta^\Upsilon|\})^2 \quad (20)$$

$${\sigma_{LN}}^2 = \int_0^\infty (\beta^\Upsilon)^2 f_\beta(\beta^\Upsilon)d\beta^\Upsilon - (\int_0^\infty \beta^\Upsilon f_\beta(\beta^\Upsilon)d\beta^\Upsilon)^2 \quad (21)$$

$${\sigma_{LN}}^2 = \int_0^\infty \frac{\beta^\Upsilon}{\sqrt{2\pi\sigma^2}}\exp\left(-\frac{(\ln(\beta^\Upsilon - m))^2}{2\sigma^2}\right)d\beta^\Upsilon - (\int_0^\infty \frac{1}{\sqrt{2\pi\sigma^2}}\exp\left(-\frac{(\ln(\beta^\Upsilon - m))^2}{2\sigma^2}\right)d\beta^\Upsilon)^2 \quad (22)$$

Let $a = \frac{1}{\sqrt{2\pi\sigma^2}}$, $b = \frac{1}{2\sigma^2}$ and $\mathrm{erf}(\beta^\Upsilon) = \frac{2}{\sqrt{\pi}}\int_0^\infty e^{-z^2}dz$

$${\sigma_{LN}}^2 = \frac{\sqrt{\pi}a\, e^{\frac{1}{b}+2m}}{2\sqrt{b}}\mathrm{erf}\left(\frac{-bm+blog(\beta)-1}{\sqrt{b}}\right)|_0^\infty - (\frac{\sqrt{\pi}a\, e^{\frac{1}{4b}+m}}{2\sqrt{b}}\mathrm{erf}\left(\frac{-2bm+blog(\beta)-1}{2\sqrt{b}}\right)|_0^\infty)^2 \quad (23)$$

This article has been accepted for publication in a future issue of this journal, but has not been fully edited. Content may change prior to final publication.

$$\sigma_{LN}{}^2 = \frac{\sqrt{\pi}a\, e^{\frac{1}{b}+2m}}{\sqrt{4b}} - \left(-\frac{\sqrt{\pi}a\, e^{\frac{1}{b}+2m}}{\sqrt{4b}}\right) - \left(\frac{\sqrt{\pi}a\, e^{\frac{1}{4b}+m}}{\sqrt{4b}} - \left(-\frac{\sqrt{\pi}a\, e^{\frac{1}{4b}+m}}{\sqrt{4b}}\right)\right)^2 \quad (24)$$

$$\sigma_{LN}{}^2 = \frac{\sqrt{\pi}\sqrt{2\sigma^2}}{\sqrt{2\pi\sigma^2}} e^{2\sigma^2+2m} - \left(\frac{\sqrt{\pi}\sqrt{2\sigma^2}}{\sqrt{2\pi\sigma^2}} e^{\frac{2\sigma^2}{4}+m}\right)^2 \quad (25)$$

$$\sigma_{LN}{}^2 = e^{2\sigma^2+2m} - \left(e^{\left(\frac{\sigma^2}{2}\right)+m}\right)^2 \quad (26)$$

$$\sigma_{LN}{}^2 = e^{2m}\left(e^{2\sigma^2} - e^{\sigma^2}\right) \quad (27)$$

3.3 Receiver

The extraction of $\mathcal{N}_{cp}$ samples of OFDM carrier and then running an FFT operation will produce the received signal in the frequency domain. This mathematical operation facilitates the conversion of the signal o the frequency domain from the time domain to the frequency domain. The Eq. (14) represents the complex signal at the receiver, which may be represented in the frequency domain as follows:

$$Y^I + jY^Q = (Z^I + jZ^Q).(X^I + jX^Q) + U^I + jU^Q \quad (28)$$

In the frequency domain, the symbols Y, Z, X, and U represent the following entities: Y denotes the complex signal, Z represents the complex fading channel's transfer function, X stands for the complex modulated signals, and U signifies the AWGN [39]. As per the CLT, the real component and the imaginary part's distributions tend to approximate a Gaussian distribution subsequent to the FFT operation[49-50]. The mean of these distributions is zero, but the variance is based on the specific channel used. In the context Rayleigh fading channel, the PDF (Z^I) and the PDF (Z^Q) may be represented as (16) and (17). In the context of the Lognormal Fading Channel, the probabilities $P(Z^I)$and $P(Z^Q)$ may be mathematically represented as,

$$f_Z(Z^I) = \frac{1}{\sqrt{2\pi\sigma_{LN}^2}} \exp\left(-\frac{(Z^I)^2}{2\sigma_{LN}^2}\right), \quad 0 \le Z^I < \infty \quad (29)$$

$$f_Z(Z^Q) = \frac{1}{\sqrt{2\pi\sigma_{LN}^2}} \exp\left(-\frac{(Z^Q)^2}{2\sigma_{LN}^2}\right), \quad 0 \le Z^Q < \infty \quad (30)$$

Where σ_{LN}^2 is the variance of the lognormal fading channel as previously derived Eq. (24). Therefore, It is evident the amplitude of the channels frequency response, denoted as |Z|, follows the Rayleigh distribution in the frequency response for previous channels. This may be mathematically represented as $|Z|=\sqrt{(Z^I)^2 + (Z^Q)^2}$.

When ISI is greater than noise, the ZF equalizer linear technique that inverts the frequency response of that channel to recover the transmitted signal. Consequently, the signal received in Eq. (28) may be equalized by performing division on both sides of that equation using $(1/\mathcal{H})$. In a M-QAM scheme, the received signal that complex and noisy is represented as Y in the frequency domain, while the collection of all feasible modulated symbols X is indicated as C, where C = {C_1, C_2, C_3, ……,C_M}. Finally, decoding algorithm of NR-LDPC codes has been suggested to be accomplished by the use of adaptive LMS decoding techniques. In order to enhance the precision of the soft bits that are sent throughout the iterative decoding process in Eq. (11).

The BER in the AWGN may be expressed as

$$P_b^{AWGN} = \frac{1}{2} erfc\left(\sqrt{\frac{E_b}{No}}\right) \quad (31)$$

If M is the square number and $M = 2^k$ =, then the BER for M-QAM is:

$$P_b^{AWGN} = \frac{1}{\log_2\sqrt{M}} \sum_1^{\log_2\sqrt{M}} P_b(k) \quad (32)$$

where [51],

$$P_b(k) = \frac{1}{\sqrt{M}} \sum_{i=0}^{(1-2^{-k})\sqrt{M}-1} \left[(-1)^{\left\lfloor \frac{i.2^{k-1}}{\sqrt{M}} \right\rfloor} \cdot \left(2^{k-1} - \frac{i.2^{k-1}}{\sqrt{M}} - 1\right) . \operatorname{erfc}\left((2.i+1)\sqrt{\frac{3(\log_2 M).r}{2(M-1)}}\right)\right] \quad (33)$$

Expanding $P_b(k)$is possible at $i = 1,2,\ldots(1-2^{-k}).\sqrt{M}-1$. In order to get increased efficiency,

$$P_{b(64QAM)}^{AWGN} = \frac{7}{12} Q\left(\sqrt{\frac{2E_b}{N_0}}\right) \quad (34)$$

Eq. (34) can be expressed in terms of erfc (),as

$$P_{b(64QAM)}^{AWGN} = \frac{7}{24} erfc\left(\sqrt{\frac{E_b}{7No}}\right) \quad (35)$$

$$P_{b(256QAM)}^{AWGN} = \frac{15}{64} erfc\left(\sqrt{\frac{4E_b}{85No}}\right) \quad (36)$$

4. BER COMPUTATION OVER LOG-NORMAL CHANNEL

In order to estimate the BER in AWGN for QAM-OFDM system under impact of log-normal fading channel. The ratio of actual bit energy to noise is, $SNR = \beta_b = \frac{|Z|^2 E_b}{N_0}$. Consequently, for a certain value of Z, the bit error conditional probability is

$$P_{b|Z} = \frac{1}{2} erfc\left(\sqrt{\beta_b}\right) \quad (37)$$

Based on our analysis of the chi-square random variable, it can be inferred that a Rayleigh distributed random variable has two degrees of freedom, and can be expressed as,

$$p(\beta_b) = \frac{1}{E_b/2\sigma_u{}^2} e^{\frac{\beta_b}{E_b/2\sigma_u{}^2}} \quad \beta_b \ge 0 \quad (38)$$

$$P_b^{\text{Log-normal}} = \int_0^\infty \frac{1}{2} erfc\left(\sqrt{\beta_b}\right) p(\beta_b) d\beta_b = \int_0^\infty \frac{1}{2} erfc\left(\sqrt{\beta_b}\right) \frac{1}{E_b/2\sigma_u{}^2} e^{\frac{\beta_b}{E_b/2\sigma_u{}^2}} d\beta_b$$

$$P_b^{\text{Log-normal}} = \frac{1}{2}\left[1 - \left(\frac{\sqrt{\sigma_{LN}^2 \frac{E_b}{2\sigma_u{}^2}}}{\sqrt{1+\sigma_{LN}^2 \frac{E_b}{2\sigma_u{}^2}}}\right)\right] \quad (39)$$

This article has been accepted for publication in a future issue of this journal, but has not been fully edited. Content may change prior to final publication.

5. NUMERICAL SIMULATION AND PERFORMANCE

The focus of this research is to assess a proposed system's performance NR-LDPC-QAM-OFDM in terms of BER across communication channels. Specifically, we investigate the lognormal fading channel. The suggested system's performance assessment is compared to that of an uncoded QAM-OFDM system. Fig. 4 presents a comparison process of BER performance between $BG1$ and $BG2$ for LDPC code. The initial coding rates were set at 1/2 for two distinct block lengths, specifically 3840 and 4928. And later they were fixed at (1/3) for the identical code lengths. The BER results of two systems are compared with the results of a Monte Carlo simulation and a theoretically determined BER that was calculated using Eq.(28). It can be shown in Fig.4, that the $BG1$-NR-LDPC - COFDM outperforms the $BG2$-NR-LDPC COFDM LDPC-COFDM for long block length by 0.95 dB at BER=10^{-5} , in the scenario when the rate is 1/3. and provide coding gain about 11.4 dB compared to uncoded QAM–OFDM scheme.

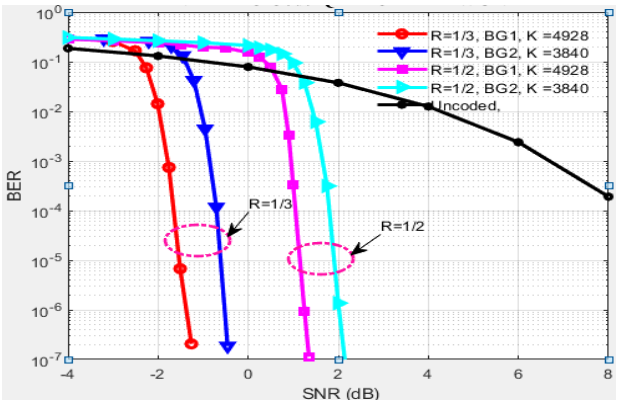

Fig. 4. BER of LDPC- COFDM for two scenarios with AWGN.

When employing different modulation techniques, Fig. 5 demonstrates the BER vs. SNR curve for a message consisting of 4928 bits. While the modulation methods are performed, 4QAM, 16QAM, 64QAM, 256QAM, and 1024QAM are supported. The findings obtained indicate that the 4QAM modulation technique exhibits superior performance when compared to the simulations that have been carried out.

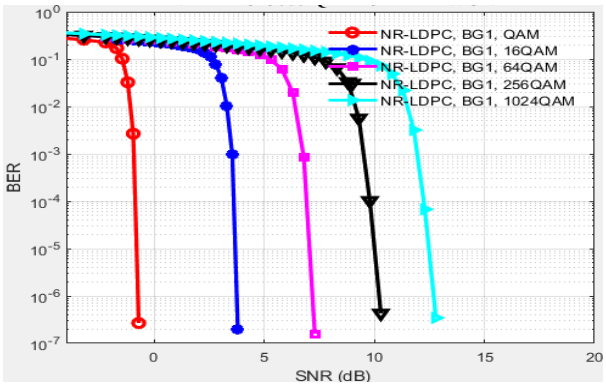

Fig.5. BER of LDPC- COFDM system based scenarios involving M-QAM with AWGN.

The estimation of variances in the AWGN channel model is carried out by utilizing SNR measurements. The AWGN channel block that had been employed previously accompanied a fading channel block in the presence of a fading scenario.

Figs. 6 and 7 illustrate the performance analysis of the NR-LDPC-QAM-OFDM system for $BG1$ at both code rates (1/2, and 1/3), in comparison to the performance of the UOFDM technique in terms of BER, under the influence of a lognormal fading channel. In contrast to SPA and MSA, the layered MS technique has been used for decoding, and success has been achieved with less iterations.

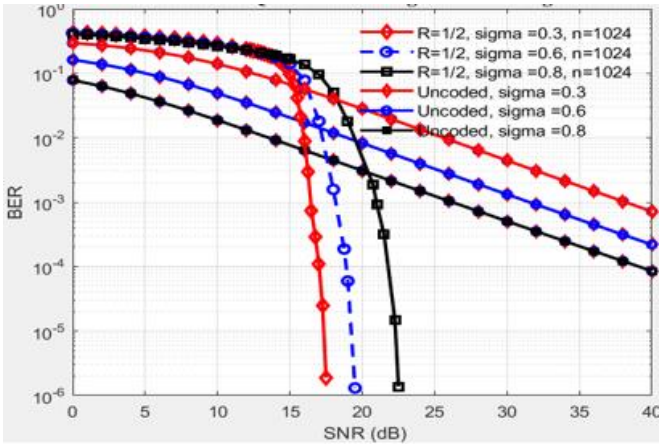

Fig.6. BER of NR- LDPC- COFDM-QAM systems over lognormal fading channel for BG1 at R=1/2

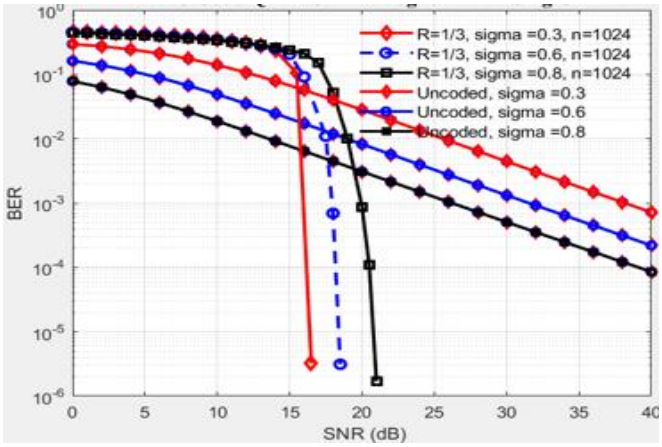

Fig.7. BER of NR-LDPC- COFDM-QAM systems over lognormal fading channel for BG1 at R=1/3

The performance analysis of the NR-LDPC Code-QAM-OFDM proposed system, including both rates (1/2 and 1/3), for $BG2$ is illustrated in Figs. 8 and 9, and the system's performance under the impact of a lognormal fading channel is shown in these Figures. The results of this analysis are evaluated in relation to the UOFDM system's performance under different value of sigma.

The simulation demonstrates a close alignment between the theoretical BER and the real BER for Uncoded OFDM across

This article has been accepted for publication in a future issue of this journal, but has not been fully edited. Content may change prior to final publication.

a Lognormal channel fading scenario. It is evident that within the lower SNR range of 0 to 10.5 dB, the systems using NR-LDPC codes exhibit worse performance compared to those without any coding scheme. This is justified by the fact that the SNR is low enough, yielding in a rather yielding in a rather high rate of error. Consequently, attempting error correction would be counterproductive. However, the performance of average BER in QAM -OFDM systems has been significantly enhanced in the higher SNR area by the utilizing of LDPC codes.

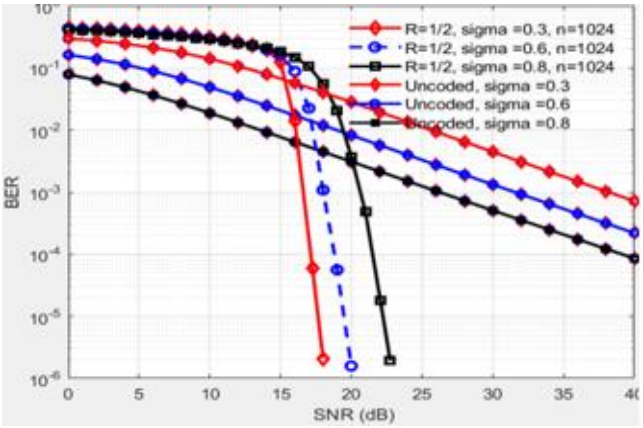

Fig.8. BER of NR-LDPC- COFDM systems over Lognormal fading channel for BG2 at R=1/2

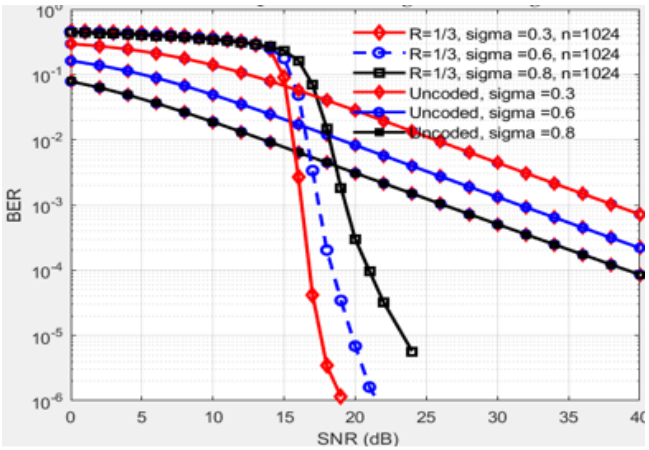

Fig.9. BER of NR-LDPC -COFDM system over lognormal fading channel for BG2 at R=1/3

Our findings clearly confirm the effectiveness of the newly constructed Layered Min-Sum Detector, as shown in Fig. 1. Comparative investigations show that this detector outperforms traditional approaches, especially in lognormal fading conditions seen in urban and suburban environment. The use of developed layered method enables more efficient processing and improved error correction, resulting in a significant boost in system performance. Results shown in simulation reveal a significant drop in bit error rates when compared to the standard models, indicating the improved capabilities of our novel detection approach.

A tabular comparison is presented, summarizing the stated investigations based on the kind of decoder, the BER with SNR, code gain, and modulation type described in Table 1.

TABLE1. Comparison results of different publications

Reference	Channel Model	Decoder	BER/FER vs SNR	Modulation
[52]	AWGN	LDPC (Min-Sum)	0.096173 at 1dB	BPSK
[2]	AWGN	LDPC (Sum Product)	10^-4 at 1ddB	QPSK
[53]	Flat Rayleigh Fading with CSI TR	LDPC(EXIT)	10^-4 at -0.7dB	16QAM (Anti-Gray)
[53]	Flat Rayleigh Fading with CSI TR	LDPC(EXIT)	10^-4 at -0.32dB	16QAM (Gray)
[54]	AWGN	LDPC(BP-OSD)	10^-4at 5dB	-
[38]	Rayleigh Fading	LMS	10^-4at 9dB	QAM-OFDM
[38]	Nakagami-m	LMS	10^-4at 7dB	QAM-OFDM

6. CONCLUSIONS

The multipath fading channel is taken into account in this research while evaluating how well the NR- LDPC- OFDM system performs. The lognormal fading channel is used in order to include the many phenomena that lead to signal distortion inside the channel. By means of Monte Carlo simulations, we observed that the QAM constellation in an NR-LDPC-COFDM has been enhanced in term. of coding gain in comparison to the uncoded OFDM system. This improvement is achieved by using the Log- Likelihood Ratio (LLRs) calculated from the PDFs of the noise created at the output of the Zero Forcing(ZF) equalizer in the fading scenario of channels. Moreover, it has been shown that the LDPC- COFDM system, when combined with LMS decoding techniques, has superior performance compared to other algorithms.

In simulations of the QAM- NR-LDPC-COFDM system operating in AWGN over the LFC, a range of standard deviations (sigma= 0.3, 0.6, and 0.8) have been evaluated, the findings demonstrate that for higher values of SNR, the LFC has better coding gain than the other fading channels as sigma decreases. For example, it can be seen that the use of the proposed QAM-LDPC- OFDM when using BG1 results in a coding gain of about 23.1 dB and 22,3 at rate (1/3) and rate (1/2) respectively, higher than that of uncoded OFDM, considering BER of around 10^{-3} in the case of (sigma= 0.3). In addition, the use of LMS decoding algorithm has been shown to significantly decrease the BER of the system. In the end, it is found that NR-LDPC code has the ability to improve the system's BER performance in the multipath fading channel. Therefore, To get a BER of 10^{-6}, it is necessary to use LDPC code with LMS technique decoding.

REFERENCES

[1] W. Ji, Z. Wu, K. Zheng, L. Zhao and Y. Liu, “Design and Implementation of a 5G NR System Based on LDPC in Open Source SDR,” in *2018 IEEE Globecom Workshops (GC Wkshps)*, Abu Dhabi, United Arab Emirates, 2018, pp. 1-6, doi: 10.1109/GLOCOM W. 2018.8644263.

[2] T. Richardson and S. Kudekar, “Design of Low-Density Parity Check Codes for 5G New Radio,” *in IEEE Communications Magazine*, vol. 56, no. 3, pp. 28-34, March 2018, doi: 10.1109/MCOM. 2018. 1700839.

This article has been accepted for publication in a future issue of this journal, but has not been fully edited. Content may change prior to final publication.

[3] R. G. Gallager, ‘‘Low-density parity-check codes,’’ in *IRE Trans. Inf. Theory*, vol. 8, no. 1, pp. 21–28, Jan. 1962.

[4] W. E. Ryan, “An introduction to LDPC codes,” in *CRC Handbook for Coding and Signal Processing for Magnetic Recording Systems*, B. Vasic, Ed. Boca Raton, FL, USA: CRC Press, 2004, Ch. 36.

[5] Y. Fang, G. Bi, Y. L. Guan and F. C. M. Lau, “A Survey on Protograph LDPC Codes and Their Applications,” in *IEEE Communications Surveys & Tutorials*, vol. 17, no. 4, pp. 1989-2016, Fourth quarter 2015, https://doi: 10.1109/COMST.2015.2436705.

[6] IEEE Standard for Information Technology--Telecommunications and Information Exchange between Systems - Local and Metropolitan Area Networks--Specific Requirements, “Part 11: Wireless LAN Medium Access Control (MAC) and Physical Layer (PHY) Specifications,” Redline,” in *IEEE Std 802.11-2020* , vol., no., pp.1-767, 26 Feb. 2021, doi: 10.1109/ IEEESTD. 2021. 9363693.

[7] A. Television and S. Committee, “ATSC Standard : Physical Layer Protocol(A/322),” no., pp.1-263, Dec., 2018.

[8] ETSI - EN 302 755, “Digital Video Broadcasting (DVB); Frame structure channel coding and modulation for a second generation Digital Terrestrial Television Broadcasting System (DVB-T2),” pp.1-188,. Jul., 2015.

[9] J. Song, C. Zhang, K. Peng, J. Wang, C. Pan, F. Yang, J. Wang, H. Yang, Y. Xue, Y. Zhang, and Z. Yang, ‘‘Key technologies and measurements for DTMB—A system,’’ in *IEEE Trans. Broadcast*., vol. 65, pp. 53–64, Mar. 2019.

[10] J. Malhotra, “Investigation of Channel Coding Techniques for High Data Rate Mobile Wireless Systems,” *International Journal of Computer Applications*, vol. 115, no. 3, pp. 39–45, 2015.

[11] W. Sułek, “The design of structured LDPC codes with algorithmic graph construction,” *Bull. Pol. Acad. Sci. Tech. Sci.*, vol. 70, no. 4, pp. 1–8, 2022, doi: 10.24425 /bpasts. 2022.141592.

[12] R. Hema, A. Ananthi, and D. C. Diana, “Coded GFDM with decision feedback equaliser for enhanced perform ance in underwater wireless optical communication,” *Opto-Electronics Review*, vol. 32,no.1, pp. 1–14 2024. https: //doi: 10.244 25/ opelre.2024. 148697.

[13] G. A. Al-Rubaye, C. C. Tsimenidis, and M. Johnston, “Performance evaluation of T-COFDM under combined noise in PLC with log-normal channel gain using exact derived noise distributions,” *IET Commun.*, vol. 13, no. 6, pp. 766–775, 2019, doi: 10.1049/iet-com.2018.6185.

[14] D. S. Shafiullah, M. R. Islam, M. Mostafa, A. Faisal and I. Rahman, "Optimized Min-Sum decoding algorithm for Low Density PC codes," in *2012 14th International Conference on Advanced Communication Technology (ICACT)*, 2012, pp. 475-480.

[15] W. Zhou and M. Lentmaier, “Generalized two-magnitude check node updating with self-correction for 5G LDPC codes decoding,” in *Proc. 12th Int. ITG Conf. Syst., Com mun. Coding, Rostock, Germany*, Mar. 2019, pp. 1–6.

[16] M.K. Roberts, R. A. Jayabalan, “Modified Optimally Quantized Offset Min-Sum Decoding Algorithm for Low-Complexity LDPC Decoder,” *Wireless Pers Communications*, vol. 80, pp.561–570, 2015, doi: org/10. 1007/s11277-014-2026-2.

[17] D. D. kumar, R. S. Selvakumari, “Performance analysis of Min-Sum based LDPC decoder architecture for 5G new radio standards,” *Materials Today: Proceedings,62* 2022, pp. 4965-4972. https:// doi. org/ 10.1016/ j.matpr. 2022.03.693.

[18] K. Sun and M. Jiang, “A hybrid decoding algorithm for low-rate LDPC codes in 5G,” in *Proc. 10th Int. Conf. Wireless Communications. Signal Process. (WCSP)*, Hangzhou, China, Oct. 2018, pp. 1–5.

[19] X. Wu, M. Jiang, and C. Zhao, “Decoding optimization for 5G LDPC codes by machine Learning,” *IEEE Access*, vol. 6, pp. 50179–50186, 2018.

[20] S. Enoch and I. Otung, “Performance Improvements in SNR of a Multipath Channel Using OFDM-MIMO,” *International Journal of Electronics and Telecommunic- ations*, vol. 69, no. 4, pp. 769–773, 2023, doi: 10.24425/ ijet.2023.147700.

[21] M. H. Ali, G. A. Al-rubaye, “Performance Evaluation of 5G New Radio Polar Code over Different Multipath Fading Channel Models,” *International Journal of Intelligent Engineering and Systems*, vol. 17, no. 2, pp. 439–452, 2024, doi: 10.22266/ijies2024.0430.36.

[22] S. Enoch and I. Otung, “Performance Improvements in SNR of a Multipath Channel Using OFDM-MIMO,” *International Journal of Electronics and Telecommunications*, vol. 69, no. 4, pp. 769–773, 2023, doi: 10.24425/ijet. 2023. 147700.

[23] Z. Yu, T. Lu, W. Zheng, H. Feng Z. Ma, and F. Zhu, “Novel memory efficient LDPC decoders for beyond 5G,” *Physical Communication*, vol. 51, 2022, 101538. https://doi.org/10.1016/j.phycom.2021.101538

[24] V. Vasylenko, S. Zaitsev, Y. Tkach, O. Korchenko, R. Ziubina, and O. Veselska, “Method of assessing the information reliability of in 5G wireless transmission systems,” *International Journal of Electronics and Telecommunication*, vol. 70, no. 1, pp. 205–210, 2024, doi: 10.24425/ijet.2024.149532.

[25] C. Zhang, X. Mu, J. Yuan, H. Li and B. Bai, “Construction of Multi-Rate Quasi-Cyclic LDPC Codes for Satellite Communications,” in *IEEE Transactions on Communications*, vol. 69, no. 11, pp. 7154-7166, Nov. 2021, doi: 10.1109/ TCOMM. 2021.3107578.

[26] F. Hamidi-Sepehr, A. Nimbalker and G. Ermolaev, “Analysis of 5G LDPC Codes Rate-Matching Design,” in *IEEE 87th Vehicular Technology Conference (VTC Spring)*, Porto, Portugal, 2018, pp. 1-5, doi: 10.1109/VTCSpring.2018.8417496.

[27] Multiplexing and Channel Coding, document TS 38.212 V15.0.0, 3GPP, Dec. 2018.

[28] M. Soszka, “Fading Channel Prediction for 5G and 6G Mobile,” *International Journal of Electronics and Telecommunications*, vol. 68, no. 1, pp. 153–160, 2022, doi: 10.24425/ijet.2022.139863.

[29] V. L. Petrović, D. M. El Mezeni, and A. Radošević, “Flexible 5g new radio ldpc encoder optimized for high hardware usage efficiency,” *Electronics*, vol. 10, no. 9, 2021, doi: 10.3390/electronics10091106.

[30] O. Bancalo. G. Kolm ban, D. Declercq, and V. Savin, “Code-design density for efficient layered LDPC decoders with bank memory organization,”. *Microprocessors and Microsystems*: 63 , 216-225, Nov. 2018. doi.org/10.1016/ j.micpro.2018.09.011.

[31] T. Thi, B. Nguyen, T. N. Tan, and H. Lee, “Efficient QC-LDPC Encoder for 5G New Radio,”*Electronics*,vol.8(6), pp.1-15,2019, doi: 10.3390/electronics8060668.

[32] H. Cui, F. Ghaffari, K. Le, D. Declercq, J. Lin and Z. Wang, “Design of High-Performance and Area-Efficient Decoder for 5G LDPC Codes,” in *IEEE Transactions on Circuits and Systems I: Regular Papers*, vol. 68, no. 2, pp. 879-891, Feb. 2021, doi: 10.1109/TCSI .2020. 3038887.

[33] Y. Wang, M. Jiang and X. Ma, “Transmitting Extra Bits With Cyclically Shifted LDPC Codes,” in *IEEE Wireless Communications Letters*, vol. 10, no. 12, pp. 2824-2827, Dec. 2021, doi: 10.1109/LWC.2021.3118675.

[34] J. V. Wonterghem , A. Alloum, J. J. Boutros c ,and M. Moeneclaey , “On short-length error-correcting codes for 5G-NR,” *Ad Hoc Networks*,vol. 79, 2018, pp. 53-62, https://doi.org/10.1016 /j.adhoc .2018.06.005.

[35] J. Xie., L. Yin, N. Ge., & J. Lu. “Improved layered min-sum decoding algorithm for low-density parity check codes,” in *9th WSEAS international conference on multimedia systems & signal processing*, 2009 , pp. 102–107.

[36] J. Nadal and A. Baghdadi, “Parallel and Flexible 5G LDPC Decoder Architecture Targeting FPGA,” in *IEEE Transactions on Very Large Scale Integration (VLSI) Systems*, vol. 29, no. 6, pp. 1141-1151, Jun. 2021, doi: 10.1109/TVLSI.2021.3072866.

[37] N. Kumar , D. Kedia, & G. Purohit, “A review of channel coding schemes in the 5G standard,” *Telecommunication Systems*, vol. 83, pp. 423–448 ,2023. https://doi.org/ 10.1007 / s11235-023-01028-y

[38] M. H. Ali, and G. A. Al-rubaye “Performance Analysis of 5G New Radio LDPC over Different Multipath Fading Channel Models,” *International Journal of Computer Network and Information Security*, vol. 15, no. 4, pp. 1–12, 2023, doi: 10.5815/ijcnis.2023.04.01.

[39] H. Zarrinkoub, “*Understanding LTE with MATLAB: from mathematical foundation to simulation, performance evaluation and implementation*,” John Wiley & Sons, Ltd, 2014.

[40] M. Nakagami. “The m-distribution - A General Formula of Intensity Distribution of Rapid Fading,” *In W. C. Hoffman: Statistical Methods of Radio Wave Propagation*,” 1960, pp 3-36. https://doi.org/10.1016/ B978-0-08-009306-2.50005-4

[41] D. V. Ha, T. T. Huong, and N. T. Hai, “Performance Investigation of High-Speed Train OFDM Systems under the Geometry-Based Channel Model,” *Intl Journal of Electronics and Telecommunications*, vol. 67, no. 3, pp. 451–457, 2021, doi: 10.24425/ijet.2021.137833.V.

[42] G. A. Al-rubaye, “Performance of 5G NR-polar QAM-OFDM in nonlinear distortion plus Non-Gaussian noise over Rayleigh fading channel,” *AEUE - Int. J. Electron. Commun.*, vol. 171, no. July, p. 154929, 2023, doi: 10.1016/j.aeue.2023.154929.

This article has been accepted for publication in a future issue of this journal, but has not been fully edited. Content may change prior to final publication.

[43] C. Xiao, Y. R. Zheng and N. C. Beaulieu, "Statistical simulation models for Rayleigh and Rician fading," in *IEEE International Conference on Communications, 2003. ICC '03*. Anchorage, AK, USA, 2003, pp. 3524-3529 vol.5, doi: 10.1109/ ICC .2003.1204109.

[44] N. Quoc-tuan, D. Nguyen, and L. S. Cong, "A 10-state model for an AMC scheme with repetition coding in mobile wireless networks," *J Wireless Com Network* , pp. 1–15, Sep.2013. https://doi.org/ 10.1186 /1687-1499-2013-219.

[45] H. Suzuki, "A statistical model for urban radio propagation," in *IEEE Transactions on Communications*, vol. 25(7), pp. 673-680, Jul. 1977. doi: 10.1109 /TCOM.1977.1093888

[46] M. K. Simon, "*Digital Communication over Fading Channel*" Second Edition. John Wiley & Sons, INC., Publication, 2005.

[47] A. Laourine, A. Stephenne and S. Affes, "On the capacity of log-normal fading channels, " in *IEEE Transactions on Communications*, vol. 57, (6), pp. 1603-1607, Jun. 2009, doi: 10.1109/TCOMM. 2009.06.070109.

[48] F. Heliot, X. Chu, R. Hoshyar and R. Tafazolli, "A tight closed-form approximation of the log-normal fading channel capacity," in *IEEE Transactions on Wireless Communications*, vol. 8,(6), pp. 2842-2847, June 2009, doi: 10.1109/TWC.2009.080972.

[49] K. Sun and M. Jiang, "A Hybrid Decoding Algorithm for Low-Rate LDPC codes in 5G," in *2018 10th International Conference on Wireless Communications and Signal Processing (WCSP)*, Hangzhou, China, 2018, pp. 1-5, doi: 10.1109/WCSP.2018.8555597.

[50] B. Tahir, S. Schwarz and M. Rupp, "BER comparison between Convolutional, Turbo, LDPC, and Polar," codes," in *24th International Conference on Telecommunications (ICT)*, Limassol, Cyprus, 2017, pp. 1-7, doi: 10.1109/ICT.2017.7998249.

[51] J. Lu, K. B. Letaief, J. C. -I. Chuang and M. L. Liou, "M-PSK and M-QAM BER computation using signal-space concepts," in *IEEE Transactions on Communications*, vol. 47, no. 2, pp. 181-184, Feb. 1999, doi: 10.1109/ 26. 752121.

[52] D. Dinesh and R. S. Selvakumari, "Materials Today : Proceedings Performance analysis of Min-Sum based LDPC decoder architecture for 5G new radio standards," in *Mater. Today Proc.*, vol. 62, pp. 4965–4972, 2022, doi: 10.1016/j.matpr.2022.03.693.

[53] Y. Jiang, A. Ashikhmin, and N. Sharma, "LDPC Codes for Flat Rayleigh Fading Channels with Channel Side Information," in *IEEE Trans. Commun.*, vol. 56, no. 8, pp. 1207–1213, 2008, doi: 10.1109/TCOMM .2008. 041040.

[54] L. Li, J. Xu, J. Xu, and L. Hu, "LDPC design for 5G NR URLLC & mMTC," in *Proceedings of the IEEE International Conference on Communications*,2020, pp. 1071-1076. IEEE. https://doi.org/10.1109/ ICC40277.2020. 9148876.

.

This article has been accepted for publication in a future issue of this journal, but has not been fully edited. Content may change prior to final publication.